MM Science Journal | www.mmscience.eu
ISSN 1803-1269 (Print) | ISSN 1805-0476 (On-line)
Special Issue | ICTIMT2021
2nd International Conference on Thermal Issues in Machine Tools
April 20, 2021, Prague, Czech Republic
DOI: 10.17973/MMSJ.2021_07_2021054

ICTIMT2021-010

PART PROGRAM DEPENDENT LOSS FORECAST FOR ESTIMATING THE THERMAL IMPACT ON MACHINE TOOLS

E. Wenkler[1,2]*, A. Hellmich[2], S. Schroeder[1], S. Ihlenfeldt[1,2]

[1]Technische Universität Dresden, Institute for Machine Tools and Control Engineering, Dresden, Germany

[2]Fraunhofer Institute for Machine Tools and Forming Technology IWU, Dresden, Germany

*Corresponding author; e-mail: eric.wenkler@tu-dresden.de

Abstract
During machining occurring losses conduct into the machine tool and lead to deformations that impair the machining accuracy. Thus, high effort is invested into the compensation of thermo-elastic errors. One new approach is to use the information extractable from part programs in combination with CNC controller systems to forecast occurring losses in terms of a look ahead function. The method allows the evaluation of part programs with respect to its thermal influence on the machine tool. Therefore, the method is applied on selected part programs, resulting loss distributions are discussed in terms of their thermal impact, and potential follow-up strategies are stated.

Keywords:
CNC; Machine tool; Thermal effects; Simulation; Thermal influence estimation; Thermal look ahead

1 INTRODUCTION

Machine tools are widely used for machining of parts due to their good balance between productivity, flexibility and accuracy. To raise the economic benefit for the user, the performance and thus the productivity of the machine tool has continuously increased. In consequence, the machine internal losses have also increased. [Grossmann 2015]

Losses occur in components and assemblies that are involved in the conversion or transmission of energy [Jungnickel 2000]. They spread in form of heat in the machine tool and lead to thermo-elastic deformations reducing its accuracy. Therefore, productivity and accuracy are always in conflict [Grossmann 2015].

To handle this conflict, different strategies are used to reduce the impact of losses and to maintain machining accuracy. A widely applied strategy is the use of cooling systems to actively cool machine tool components with significant loss emission. Current machine tools use about 1/5 of their energy consumption for cooling systems [Denkena 2011, Brecher 2010, Brecher 2016, Abele 2014, Shabi 2019]. Cause of the aim for energy efficiency the energy consumption joined the conflict of productivity and accuracy.

In order to achieve an efficient cooling, there are efforts towards decentralized cooling systems, which can be controlled individually and thus achieve a better overall tempering of the machine tool [Hellmich 2018].

Preceding remarks show that the energy consumption of cooling systems is more and more contributing to the total energy consumption of the whole machine tool. The efficient control of cooling systems is thus moving into the focus of research. This paper presents an approach that can predict the losses of the individual loss sources, depending on the machining task, which is a valuable tool for the energy-efficient control of cooling systems.

2 STATE OF THE ART

Losses have a high priority in the machine tool sector. According to current estimations, more than half of all machining errors are due to thermal problems of the machine tool [Brecher 2016]. The majority of heat sources within machine tools are caused by losses in assemblies, such as bearings, guides and motors [Jungnickel 2000, Mayr 2012, Ramesh 2000].

Measuring the losses is very complex, since sensors have to be integrated at the loss occurrence into the assembly [Kekula 2018]. Therefore the losses of the individual loss causes are examined and modelled separately, e.g. for bearings [Palmgreen 1957]. These models allow the calculation of the occurring loss depending on the operating conditions, without touching the assembly.

During machining on a machine tool, the operating conditions at the respective loss occurrences change continuously. A direct use of the loss models without considering the manufacturing task is therefore not possible.

To forecast the occurring losses for a completely manufacturing task, the resulting machine movements have to be determined and used during loss model application, which is described in this paper.

3 PLACEMENT OF THE WORK

The presented approach belongs to the project B10 of the CRC/TR 96. The goal of B10 is to research strategies for a “thermal precontrol” of machine tools. Thermal precontrol comprises loss prediction, loss patterning and the derivation of control strategies to achieve a temporally stable temperature field. Therefore the project targets at the front of the thermo-elastic chain [Hellmich 2018], to decrease changes in temperature field, deformation field and tool centre point displacement.

Fig. 1 summarizes the issue. The left branch describes the influence of a part program on the thermo-elastic deformation of machine tools. The right branch shows the modelling strategy and their usage for a determination of optimized control strategies for tempering systems. The yellow cased block in the right branch is issued in this paper. Section 4 describes the general method for the loss forecast while section 5 applies the method on selected part programs with an discussion of resulting loss distributions.

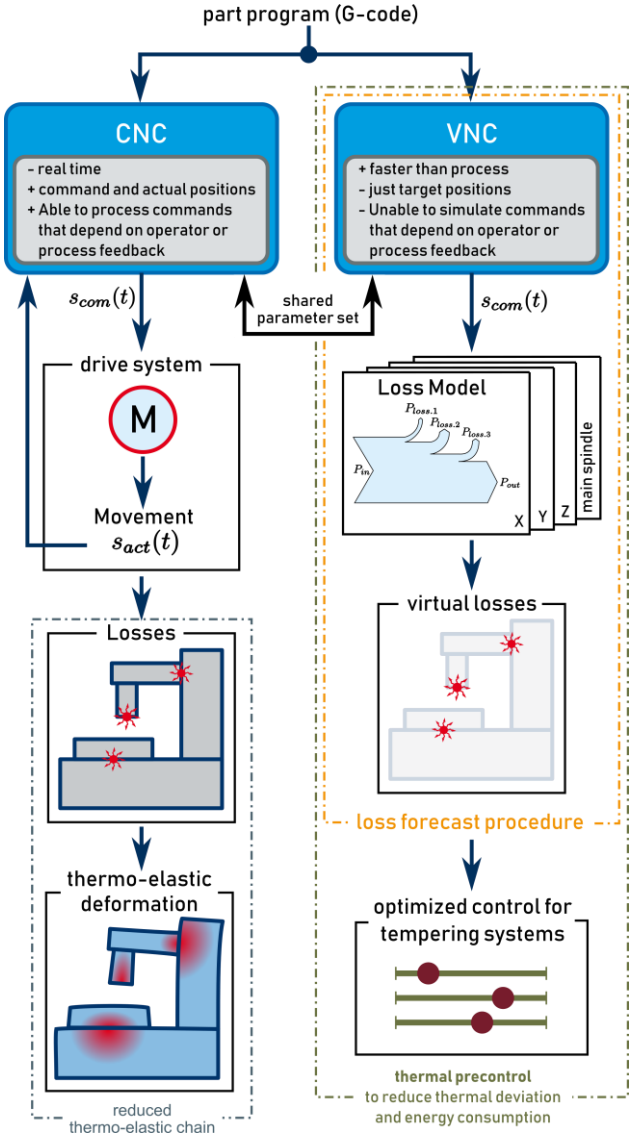

Fig. 1: Placement of the loss forecast within project B10 of the CRC/TR 96

4 METHODOLOGY FOR LOSS FORECAST

4.1 Overview

Machine tools emit different losses depending on their operation state, which is the main reason for thermal changes within the machine tool. While in non-operating mode, losses are mostly stable because the only loss sources are motors constantly influenced by gravity, like the Z-axis, active auxiliary units and hydraulic systems [Shabi 2019]. During automatic operating mode, multiple sources emit losses that strongly depend on the manufacturing task. These are for example:

- Motors
- Bearings
- Guidings

To forecast the occurring losses of a machine tool during a specific process, two major steps are to accomplish.

- First, the machining task, which is defined in the NC program, must be interpreted so that the resulting axis movements of the machine tool are known.
- Secondly, the axis-specific losses have to be calculated with the aid of the previously determined axis movement.

Fig. 2 summarizes the general workflow. The two main steps of loss prediction are discussed in the following sections 4.2 and 4.3.

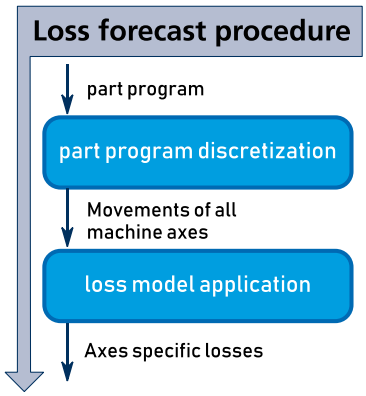

Fig. 2: General loss forecast procedure according to Fig. 1

4.2 Part program discretization

Part programs are usually generated after process planning with computer aided manufacturing systems (CAM) where resulting paths and machine commands for a desired technology are defined. The paths within part programs are relative to the raw part. They do not contain axes specific movement commands for the machine tool. With the interpretation by a CNC, the defined motion is transformed on the machine tool axes. For example, machining the same process (part program) on machines with serial and parallel kinematics results in significantly different axis movements [Ihlenfeldt 2012].

The part programs are written in G-code (also called NC-code or CNC-code) [DIN 66025-1 1983, DIN 66025-2 1983]. G-code is a programming language for machine control systems that distinguishes fundamentally in path conditions and additional functions. Despite existing standards for G-code, control systems differ in terms of path processing and additional functions. Some control manufacturers have also developed their own syntax, which however is similar to G-Code in many respects. Therefore, part programs are mostly controller specific and should be interpreted with the appropriate controller type to achieve a high correlation between simulated and real machine behavior. Due to complexity [Suk-Hwan 2008] and non-transparent internal processes, a reconstruction of the internal control processes to determine the axis movements is often not accurate enough and very time-consuming.

Since machine tool controllers are a software, running on a machine integrated computer, most control manufacturers offer the opportunity to run them offline, which is e.g. used for commissioning or collision detection and will further be called virtual numerical control (VNC). Instantiated with the axes configuration of the machine tool, this leads to high correlations between simulated and real movement.

By using the appropriate VNC, the interpolation points of the process can be calculated and transformed on the machine axes with respect of speed and jerk limits, which can further be used for the application of loss models.

It should be mentioned that the VNC cannot cover all variations in a part-program. Commands that involve the machine operator (e.g. programmed stop) or auxiliary systems coupled though the PLC (e.g. in process tool length measurement) cannot be simulated because they are outside the control's responsibility or rely on process feedback. This issue may be solved by separating the part program in operator or process dependent parts and independent parts, which will be part of further research. The major differences of a VNC and a CNC are sumarized in Fig. 1.

4.3 Loss model application

The losses of an axis strongly depend on its size and the construction. Rotatory axes mainly have losses in the bearing and the motor, while translational axes have additional losses in the guiding [Jungnickel 2000].

As mentioned in section 4.1, the losses depend on the operation state. For this purpose, models exist to describe the respective loss sources. In [Jungnickel 2010] relevant models were summarized, which are used in the CRC/ TR 96 [Schroeder 2019] and within this work.

The loss model parameterization in combination with thermal simulation models is very complex and above all iterative, as described in [Kauschinger 2015]. With parameterized models, losses of a respective loss source can be determined according to the operation state.

To determine the operating state of an axis, the machining operation has to be discretized and transformed to the axes according to the procedure in section 4.2. This results in time series of axis positions. In practice, these support points are transferred to the drives, which move quasi linearly in between. Therefore the movement from one to the next support point of the time series can be assumed to be linear. With this information, the corresponding movements in the individual loss sources can be determined, which is the main influence of the loss models. More details to used loss models and their application are given in section 5.3.

5 APPLICATION

5.1 Research object

The investigations were performed on a hexapod (see Fig. 3), which is equipped with multiple thermal sensors and used as research demonstrator in prediction, correction and compensation of thermo-elastic errors. It has six identical axes (see Fig. 4), which are all mounted on the fixed base and the moved platform. Each axes has a movement range of 0.5 m and a speed limit of 1 m/s.

The machine is controlled by a Beckhoff CNC preceded by a HexaBOF (see Fig. 5), developed at the IMD of the TU Dresden. The HexaBOF is focussing on the offline transformation, position limits, work area check and model based corrections. It has its own programming language called GEO-code that allows positioning with desired orientation in $\mathbb{R}^3$ similar to standardized commands of G-code. It generates G-Code on axis level (further called axis G-code), which is processed by the Beckhoff CNC at a cycle time of

Fig. 3: Research object: hexapod

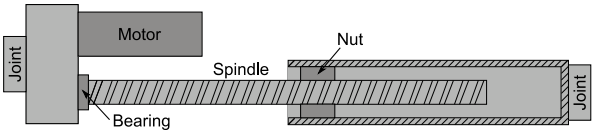

Fig. 4: schematic axis setup

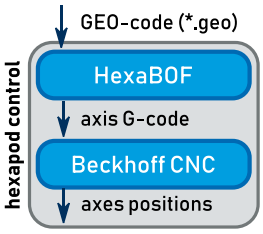

Fig. 5: real hexapod control architecture representing 'CNC' block in Fig. 1

10 ms. Due to nonlinear transformation models, the development of HexaBOF allowed the adaptability of the transformation model with low-cost, compared to the time critical implementation within the CNC. More details can be found in [Kauschinger 2006].

The hexapod is fully defined so that each axis can be moved without moving the other five axes. This allows the execution of single axis movements as well as 3/5-axis movements with and without consideration of the transformation.

5.2 VNC application for part program discretization

For the virtual processing of part programs, the in section 4.2 described procedure has to be applied for the hexapod control (see Fig. 5).

Therefore, the following key issues have emerged:

1. Creation of a converter to transform G-Code into GEO-Code
2. Connection of the HexaBOF for the offline transformation from GEO-Code to axis G-Code
3. Connection of a Beckhoff VNC for offline G-code interpretation, to receive axis positions

For the first step, a converter was developed, which accepts 3-axis machining operations as G-code and converts them into a GEO program. The conversion from GEO to axis G-code is done manually via HexaBOF. Due to the language specifics, the number of NC blocks changes during the conversion. To enable conclusions to be drawn about the original NC program, the reference to the original block was restored after each conversion step, by replacing block numbers.

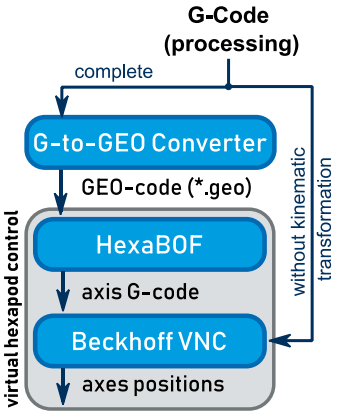

Fig. 6: VNC architecture for the hexapod

The created VNC is based on a Beckhoff library, that provides essential functions for the virtual operation of a CNC. An interface was developed via which NC programs can be processed, returning the resulting position series of all axes. The VNC is instantiated by the interface with the axis configuration of the Hexapod, which achieves a high correlation between real and virtual machine behaviour.

The developed modules were examined and validated individually and in interaction with the use of different part programs. Tests within a virtual machine showed that the virtual interpretation of the part programs is between 50 and 60 times as fast as the machining task itself. Thus, such approaches could be used efficiently during process planning.

5.3 Loss model integration and application

To predict the losses of a machine tool, parameterized loss models [Jungnickel 2010] are required as well as the current operating state of the loss source.

The operating state is mainly defined by the present speed at the loss source, which is made possible by the derivation of the position time series from section 5.2.

At the research object are three significant loss source types: bearing, ball screw drive and motor. Each loss occurs once per axis, which leads to 3*6=18 loss sources at the hexapod.

The loss models used are from [Jungnickel 2010] and were parameterized by the investigations in [Kauschinger 2015]. In the following, the models are briefly introduced.

Bearing losses

The used bearing loss model (1) is based on the research of Palmgreen [Palmgreen 1957] and divides into a hydrodynamic M_{hydro}, load dependent M_{load} and sealing loss M_{seal}.

$$M_{bearing} = M_{hydro} + M_{load} + M_{seal} \quad (1)$$

Hydrodynamic losses (2) are speed-dependent, since the lubricating film varies according to the speed. Parameters are: the bearing constant f_0, the average bearing diameter d_m, the kinematic viscosity ν and the angular speed ω.

$$M_{hydro} = 4501 \cdot f_0 \cdot {d_m}^3 \cdot (\upsilon \cdot |\omega|)^{\frac{2}{3}} \;\forall\; \upsilon\omega \geq 2000 \frac{m^2}{s^2} \quad (2)$$

The axial and radial bearing load primarily defines the load-dependent loss component (3). It is sufficient to consider only the preload since the process forces are largely cancelled out by the bearing design, as explained in [Kauschinger 2016]. Parameters are: Bearing constant f_1, axial force F_a, radial force F_r and average bearing diameter d_m.

$$M_{load} = f_1(1.4 \cdot F_a - 0.1 \cdot F_r) \cdot d_m \quad (3)$$

The used bearing is lubricated with a grease in which mineral oil is dissolved. In order to keep the grease in the bearing, sealing rings are used, which cause additional friction. Therefore an sealing loss (4) [SKF 2020] was considered which extends the model of PALMGREEN [Palmgreen 1957]. Parameters are: Coefficients for the sealing ring K_{S1} and K_{S2}, diameter of the sealing ring that is sliding over the bearing ring d_{seal} and the exponent for the sealing ring β.

$$M_{seal} = K_{S1}\left({d_{seal}}^{\beta} + K_{S2}\right) \quad (4)$$

Ball screw drive losses

Losses within the ball screw drive (5) separate into a loss caused by the rolling elements M_{roll} and an additional sealing loss M_{seal}. The sealing loss occurs for the same reasons as described for the bearing loss. Therefore (4) can be used for its calculation.

$$M_{bsd} = M_{roll} + M_{seal} \quad (5)$$

The loss caused by the rolling elements M_{roll} was used from [Jungnickel 2010], and is based on empirical research. Parameters are: Spindle diameter $d_{spindle}$, nut diameter d_{nut}, number of groves i where rolling elements are in contact, preload force F_v and the dynamic load capacity C.

$$M_{roll} = 4.52 \cdot 10^5 \cdot {d_{spindle}}^{1.44} \cdot {d_{nut}}^{1.33} \cdot i \cdot \frac{F_v}{C} \quad (6)$$

Motor losses

The motor loss model (7) used here was setup of the idea, that the motors effective torque is equivalent to the sum of loss moments. With an assumed static efficiency value η, the motor loss can be determined.

$$M_{mot} = \frac{1-\eta}{\eta}\left(M_{friction} + M_{acceleration}\right) \quad (7)$$

$$M_{friction} = M_{bearing} + M_{bsd} \quad (8)$$

In addition to the friction losses, the acceleration loss $M_{acceleration}$ is taken into account. Parameters are: Moment of inertia J, angular speed ω and the time change dt.

$$M_{acceleration} = J\frac{|\omega|}{dt} \quad (9)$$

The current motor loss model does not consider dynamic efficiency values η and process forces, since the prediction of process forces is not trivial [Hänel 2019]. Further research steps will analyze solutions for the integration of efficiency map lines $\eta = f(M, n)$, alternative models like [Winkler 2015] and process force forecast strategies like [Hänel 2019] for a more accurate forecast of motor losses.

Loss model application

The previously described loss models (1) to (9) can be applied on the resulting position time series of section 5.2. The models mainly require an angular speed ω, that can be obtained out of the position time series. Equation (10) shows the calculation of the time dependent angular speed for an axis. Parameters are: Rotational speed n, axis speed v, spindle slope s, position at a specific time $p(t)$ and the sample time dt.

$$\omega(t) = 2\pi n(t) = 2\pi\frac{v(t)}{s} = 2\pi\frac{\frac{p(t)-p(t-1)}{dt}}{s} \quad (10)$$

The angular speed is axis dependent, which leads to six different speeds. Therefore, even with identical loss models for all six axes, the losses of the axes are individual.

5.4 Loss distribution analysis

The procedure described in sections 5.2 and 5.3 can be used to predict loss moments of individual loss sources for any part program. Based on the loss moment the corresponding loss power and loss energy can be calculated with little effort (11). Parameters are: Loss energy E_{loss}, loss power P_{loss}, passed time dt and the angular speed ω.

$$E_{loss} = P_{loss} \cdot dt = M_{loss} \cdot \omega \cdot dt \quad (11)$$

The procedure was applied to three different NC programs, which are discussed separately below. These examples were chosen to validate the solution and illustrate its potential with increasing movement complexity. For simplification the focus was put on the first of the hexapods six axes and further on its motor loss. For each NC program, the resulting motor loss moments over time and the corresponding power dissipation over the NC block are shown. The presentation of the loss power over the blocks was chosen in order to allow an evaluation of individual blocks with regard to occurring losses. All time dependant graphs are additionally smoothed with a rolling window over 30s.

Linear pendulum movement

The first NC-program performs a simple linear movement ($\mathbb{R}^1$), which helps to interpret the resulting loss curves. The goal was to create obvious correlations between NC-program and resulting loss distributions.

Through the program, all six axes move simultaneously from 0 to 100 mm and back again. This movement is repeated so that the ideal movement would take 15 minutes and then the axis speed is incremented or decremented according to Fig. 7. Between the ideal and real speed is a big difference. This is caused by the limitations of path deviation and jerk. Especially at high speeds, the axis cant follow the desired path, resulting in a slower movement.

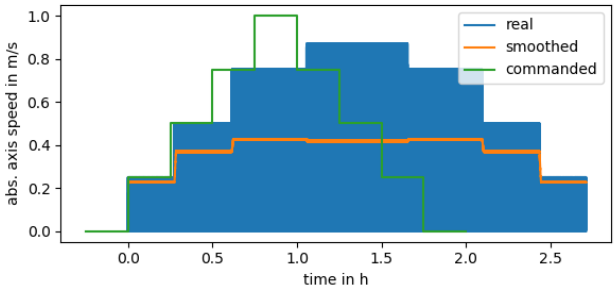

Fig. 7: absolute speed for the linear movement

Within the loss moment distribution in Fig. 8 the change of the axis speed (Fig. 7) is clearly correlating with the loss moment, which is mainly caused by the speed dependence of the friction moment (8). The corresponding loss power distribution is shown in Fig. 9. Because of the axis limitations, the changes in loss moment and average axis speed are smaller at high speeds, resulting in small changes of the loss power according to (11).

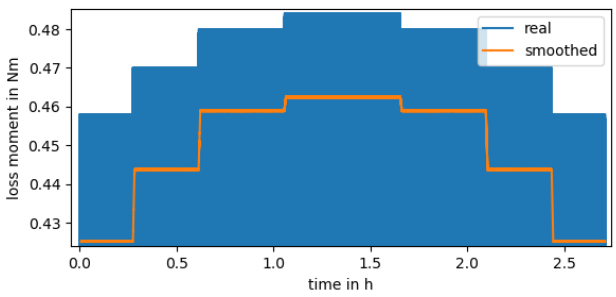

Fig. 8: Loss moment within the X-Motor

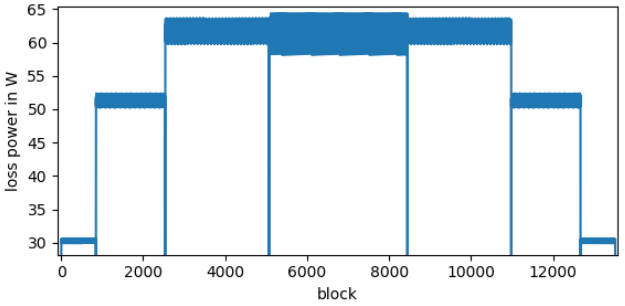

Fig. 9: X-Motor induced loss power of G-Code blocks

Cone movement

The second NC-program was created to analyze the loss model results, with continually decreasing movement under constant commanded path speed in $\mathbb{R}^3$. Compared to the first test scenario the axis limitations continuously gain on impact. The NC-program describes the movement along the surface of a cone, as shown in Fig. 10. The cones rotational axis is oriented parallel to the Z-axis and is segmented along the Z-axis, so that circular movements are done by each level. With increasing Z position the circles shrink while remaining the target path speed, which leads to stronger accelerations with rising Z position.

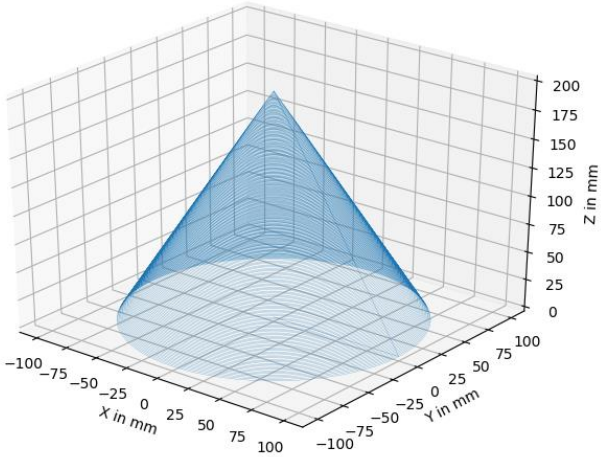

Fig. 10: Cone movement of the NC-program

At the beginning, the large circles are driven, which is represented by the area filled in at the bottom in Fig. 11 (up to 0.405 Nm). The individual spikes (approx. 0.407 Nm) are caused by the feed motion between the circles. The anomalies at the end are caused form control limitations because the machine is unable to follow the continuously decreasing circles at the desired path speed. During the real execution of the program, clear vibrations and a bouncing of the machine could be heard and seen.

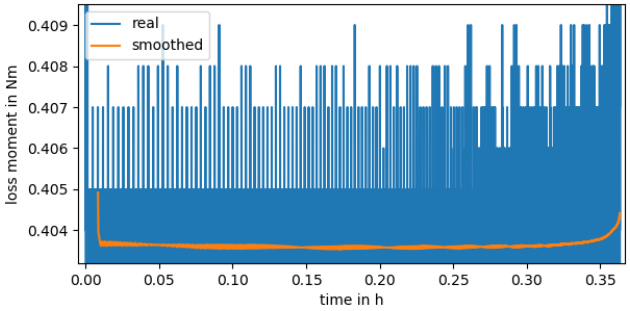

Fig. 11: Loss moment within the X-motor

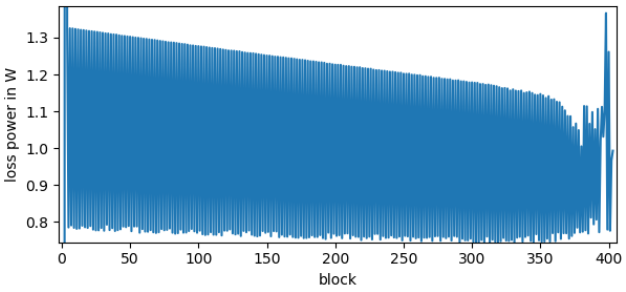

Fig. 12: X-Motor induced loss power of G-code blocks

While the loss moment increases the loss power (Fig. 12) of the block reduces because of the decreasing angular speed (11) in fact of the smaller circles.

The test scenario shows the loss forecast for a part program with continuously changing movements. The anomalies that are visible at the end of Fig. 11 and Fig. 12 also arised at the real execution of the nc-program, which validates the simulation results.

Real manufacturing task

In a real manufacturing task, the loss curves are much more complex than those of the preceding tasks and are difficult to analyze. To illustrate this, a real manufacturing technology was used (see Fig. 13). The technology has been created according to classical technology planning, with roughing first and then finishing within the following order:

1. Plane milling
2. Bag milling
    1. Opened bag
    2. Big Bag
    3. Small Bag
3. Grove milling
    1. Long grove
    2. Short grove
4. 7x drilling

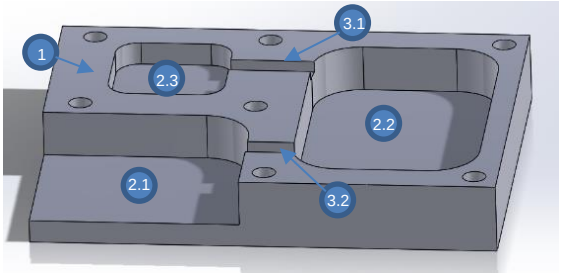

Fig. 13: Demonstration part

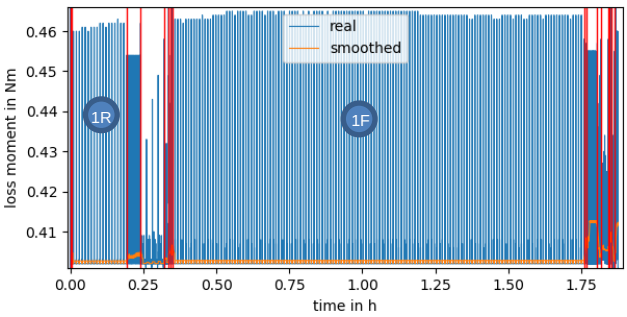

Fig. 14: Loss moment within the X-motor

Fig. 14 shows the corresponding loss moment distribution for the x-motor of the hexapod. The red vertical lines indicate a change of the operation step, like switching from plane milling to bag milling. The plane milling operations (1R: roughing and 1F: finishing) represent the two big areas

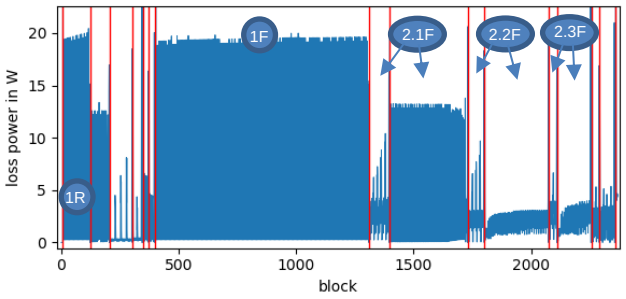

Fig. 15: X-motor induced loss power of G-code blocks

separated by the red lines. Especially the finishing operation is very time consuming, indicating inefficient cutting parameters. Additionally, there is a difference between cutting movement (at about 0.41 Nm) and positioning movement (at about 0.46 Nm) visible.

While watching on the loss power distribution at Fig. 15, the positions of the red lines change in relation to Fig. 14. This happens because of the different times a block is active, depending on defined path velocity and path length. As example the plane milling operations shrink, cause of long ways represented by a block. The impacts of a block on the emitted loss powers are clearly varying, depending on the operational task. The finishing operations 2.1 to 2.3 point to two areas, because they were separated in wall and ground finishing. With the example is shown that the resulting losses vary according to the manufacturing technology.

Summary

The predicted loss distributions strongly depend on the process. The *linear pendulum movement* showed basic correlations between the path speed and the resulting loss for an single axis movement in $\mathbb{R}^1$. In the example of *cone movement,* the path speed was fixed while continuously reducing the path length in $\mathbb{R}^3$, leading to similar effects. These examples were chosen for basic validation of the model. Within the *real manufacturing task*, the model was applied to a real process, resulting in complex loss distributions, which were described briefly.

6 SUMMARY AND CONCLUSION

The forecast of machine internal losses, depending on the part program, was described and explained at specific examples. Correlations between resulting loss moment over the time and the loss power over the sentence were focussed.

In addition, the loss energy can be determined according to equation (11), which was not further focused within the paper.

The used VNC as well as the loss models can be substituted, allowing a transfer to other machine tools, while the general procedure of the loss forecast in section 4.1 remains the same.

7 OUTLOOK

The presented loss models within section 5.3, are actually not considering the process dependant losses which mainly effect the motor loss (7). Further research has to focus on the increase of model accuracy or additional models, that may be relevant for other machines, like guide rails, environmental changes or loss emission in auxiliary units.

The loss moment (Fig. 14) and loss power (Fig. 15) distribution is valuable for the efficient control of cooling systems, since they describe the dynamic thermal load caused

from manufacturing tasks. With their help, control signals for cooling systems can be determined, which contribute to a thermally stable machine tool.

Future investigations must therefore focus on the control of cooling systems. For this purpose, limits of the cooling systems have to be considered, such as maximum cooling capacities, reaction times as well as specifics of the cooled body like the heat transfer coefficient. If the loss predictions are successfully used to control the cooling systems, two advantages are expected.

On the one hand, the energy input can be reduced because the cooling power is controlled according to the power loss and unreasoned cooling can be avoided.

On the other hand, the machine tools thermal behaviour can be improved, since power loss and cooling power correlate more strongly and thus reducing the absolute heat flow into the machine tool.

8 ACKNOWLEDGMENTS

The presented research activities are part of the project “Control data driven forward influencing the temperature field of a machine tool (thermal precontrol)” (Ref. No. CRC/TR 96, B10). The authors would like to thank the German Research Foundation (DFG) for financial support.

9 REFERENCES

Books:

[Suk-Hwan 2008] Suk-Hwan, S. et al. Theory and Design of CNC Systems. London: Springer London, 2008, ISBN 978-1-84800-335-4

Norms:

[DIN 66025-1, 1983] DIN e.V., Programmaufbau für numerisch gesteuerte Arbeitsmaschinen, Teil 1: Allgemeines, Beuth-Verlag, Berlin, 1983

[DIN 66025-2, 1983] DIN e.V., Programmaufbau für numerisch gesteuerte Arbeitsmaschinen, Teil 2: Wegbedingungen und Zusatzfunktionen, Beuth-Verlag, Berlin, 1983

Paper in a journal:

[Brecher 2010] Brecher, C., et al. Ressourceneffizienz von Werkzeugmaschinen im Fokus der Forschung: Effizienzsteigerung durch Optimierung der Technologien zum Komponentenbetrieb, wt Werkstattstechnik online, 2010, 7/8, p. 559-564

[Denkena 2011] Denkena, B., et al. Effiziente Fluidtechnik für Werkzeugmaschinen: Ermittlung und Reduktion des Energiebedarfs am Beispiel des Kühlwassersystems, wt Werkstattstechnik online, 2011, 5, p. 347–352

[Grossmann 2015] Grossmann, K., Ott, G. Introduction. In: K. Grossmann, Thermo-energetic Design of Machine Tools. Springer International Publishing, 2015, p. 1-11, ISBN 978-3-319-12625-8

[Hänel 2019] Hänel, A. et al: Development of a Method to determine Cutting Forces based on Planning and Process Data as contribution for the Creation of Digital Process Twins. MM Science Journal, 2019, Vol. 4, p. 3148-3155

[Kauschinger 2015] Kauschinger, B. and Schröder, S. Uncertain Parameters in Thermal Machine-Tool Models and Methods to Design their Metrological Adjustment Process. Applied Mechanics and Materials, 2015, Vol. 794, p. 379-386

[Mayr 2012] Mayr, J. et al: Thermal errors in machine tools. CIRP Anals, 2012, Vol. 61(2), p. 771–791

[Palmgreen 1957] Palmgreen, A. Neue Untersuchungen über Energieverluste in Wälzlagern. VDI-Berichte, Vol. 20, Düsseldorf: VDI-Verlag, p. 117-121, 1957

[Ramesh 2000] Ramesh, R. et al: Error compensation in machine tools – a critical review, Part II: thermal errors, International Journal of Machine Tools and Manufacture, 2000, Vol. 40(9), 2000, p. 1257–1284

[Schroeder 2019] Schroeder, S. et al: Identification of relevant parameters for the metrological adjustment of thermal machine models. International Journal on Interactive Design and Manufacturing, 2019, Vol. 13, p. 873-883

[Winkler 2015] Winkler, S. and Werner, R. Thermo-Energetic Motor Optimisation. In: K. Grossman, Thermo-energetic Design of Machine Tools. Springer International Publishing, 2015, p. 223–231, ISBN 978-3-319-12625-8

Paper in proceedings:

[Brecher 2016] Brecher, C. et al. Thermo Energetic Design of Machine Tools and Requirements for Smart Fluid Power Systems. In: 10. Internationales Fluidtechnisches Kolloquium, 2016, Volume 2, p. 177-194

[Hellmich 2018] Hellmich, A. et al. Analyzing and Optimizing the Fluidic Tempering of Machine Tool Frames. In: Proceedings of Conference on thermal Issues in Machine Tools, 2018, p. 195-210

[Kauschinger 2016] Kauschinger, B. and Schröder, S.: Uncer-tainties in Heat Loss Models of Rolling Bearings of Machine Tools. In: Procedia CIRP, 2016, Vol. 46, p. 107–110

[Kekula 2018] Kekula, J. et al. Investigation of passive torque of oil-air lubricated angular contact ball bearing and its modelling. In: Proceedings of Conference on Thermal Issues in Machine Tools, 2018, p. 281-290

Technical reports or thesis:

[Eberhard 2014] Eberhard, A., Tilo, S. and Martin, B. Maximierung der Energieeffizienz spanender Werkzeugmaschinen: Schlussbericht zum Projekt Maxiem. Darmstadt: Technische Universität Darmstadt, Institute of production management, technology and machine tools, 2014

[Ihlenfeldt 2012] Ihlenfeldt, S. Redundante Werkzeugmaschinenstruktur für die Komplettbearbeitung im Großwerkzeugbau. Chemnitz: Technische Universität Chemnitz, Faculty of Machine Engineering, 2012

[Jungnickel 2000] Jungnickel, G. Simulation des thermsichen Verhaltens von Werkzeugmaschinen. Dresden: Technische Universität Dresden, Institute of Mechatronic Engineering, 2000.

[Jungnickel 2010] Jungnickel, G. Simulation des thermischen Verhaltens von Werkzeugmaschinen: Simulation und Parametrierung. Dresden: Technische Universität Dresden, Institute of Mechatronic Engineering, 2010

[Kauschinger 2006] Kauschinger, B.: Verbesserung der Bewegungsgenauigkeit an einem Hexapod einfacher Bauart. Dresden: Technische Universität Dresden, Institute of Mechatronic Engineering, 2006

[Shabi 2019] Shabi, L. Thermo-energetic Optimized Fluid Systems for Machine Tools. Dresden: Technische Universität Dresden, Institute of Mechatronic Engineering, 2019

Web documents:

[SKF 2020] SKF. Das SKF Verfahren zur Berechnung des Reibungsmoments. Last check: 20.10.2020 URL: https://www.skf.com/binaries/pub41/Images/0901d196809bc183-17-0707-DE---17000-w-Apendix-1---SKF-friction-model_tcm_41-299767.pdf